materials proceedings

Proceeding Paper

Early-Age Creep and Shrinkage Properties of Printed and Cast Cement Composite †

Rihards Gailitis [1,*], Pauls Pudans [1], Krists Ziemelis [2], Girts Bumanis [2] and Andina Sprince [1]

1 Institute of Structural Engineering, Riga Technical University, Kipsalas 6A, LV-1048 Riga, Latvia
2 Institute of Materials and Structures, Faculty of Civil Engineering, Riga Technical University, Kipsalas 6A, LV-1048 Riga, Latvia
* Correspondence: rihards.gailitis@rtu.lv

† Presented at the 10th MATBUD'2023 Scientific-Technical Conference "Building Materials Engineering and Innovative Sustainable Materials", Cracow, Poland, 19–21 April 2023.

Abstract: In recent years, 3D printing has been more and more used in the development of buildings and building elements. Mostly-printed structures are subjected to compression that is oriented perpendicular to the layer laying direction. When applying load in this way, the printed structure exhibits characteristics similar to masonry structures. However, as the technology and application of 3D printing develop, the structures also become more complicated and subjected not only to direct compression but other stresses as well. In this paper, long-term properties together with compressive strength were determined for 3D-printed specimens with load applied in the same direction as the layers are laid. The long-term and mechanical properties were compared with cast same-composition specimens. Results show that for the printed specimens, the compressive strength was more than two times lower than cast specimens, while the creep properties were slightly lower for the printed specimens.

Keywords: cement composite long-term properties; 3D-printed cement composite; tensile stress

Citation: Gailitis, R.; Pudans, P.; Ziemelis, K.; Bumanis, G.; Sprince, A. Early-Age Creep and Shrinkage Properties of Printed and Cast Cement Composite. *Mater. Proc.* **2023**, *13*, 35. https://doi.org/10.3390/materproc2023013035

Academic Editors: Katarzyna Mróz, Tomasz Tracz, Tomasz Zdeb and Izabela Hager

Published: 17 February 2023

1. Introduction

Additive manufacturing, more frequently known as 3D printing, is the fabrication method of objects using a print head, nozzle, or other printer technologies to deposit material to the print surface [1]. The 3D printing process has been successfully used in many disciplines, such as aerospace, automotive, biomedical, and food industries. It is claimed to allow quicker and cheaper production of an object, especially intricate and delicate objects with complex geometry. Unlike other manufacturing means, 3D printing has a much higher automation level that further contributes to labor and cost reduction, reducing production time [2–5].

The civil engineering field also has developed to a stage where the design of the structure has become much more complex, while load-bearing necessities have not been reduced. Furthermore, to meet the demand for residential buildings as well as infrastructure objects, there is a high need to build faster and reduce building costs. There are high hopes that 3D printing, due to success in other fields, will also bear fruit in civil engineering applications. It has been estimated that 3D printing will reduce construction waste by 30 to 60%, decrease production time by 50 to 70%, and drop labor costs by 50 to 80% [6]. To show these improvements, cementitious material compositions are specifically designed to flow evenly and have proper layer adhesion to one another. Furthermore, 3D-printed concrete sections are more prone to acid attacks as well as shrinkage [7]. The weakest part of the 3D-printed section is claimed to be the layer connecting zone. They also show anisotropic behavior and insufficient insulating properties that lead to possible heat loss [8,9].

As 3D printing of structures are more frequently used to develop a structure where layers are put on top of one another and subjected to direct compression, it was predicted that the structure would work similarly to masonry structures. However, as not all the structures are subjected to direct compression, there is a need to gain data and knowledge on how printed structures act under other stresses. For instance, retaining walls have load applied on the side of them. Therefore, tensile stresses significantly affect the structure's load-bearing capacity.

This article investigates the early-age creep and drying shrinkage properties of 3D-printed cement composite that are loaded in the direction parallel to layers and cast cement composite and compares them to one another.

2. Materials and Methods

Printed beam shape specimens were prepared for tensile stress impact on printed specimens to relate creep and shrinkage property determination. Each printed specimen had four layers. They were modeled to be 40 × 40 × 1000 mm, but due to the cement composite mix flowability, the width of the specimens at the base was 83 mm, and 67 mm at the top. The used cement composite composition was similar to cement mortar. Due to the fact that the composition of the used cement composite is a trade secret, specific amounts and types of materials cannot be disclosed in this article. The mass partition of the used cement composite is shown in Table 1. The specimen printing process is shown in Figure 1.

Table 1. Used cement composite composition partitions.

Material	Partition, %
Portland cement	33
Quartz sand 0/0.4 mm	49
Water	18

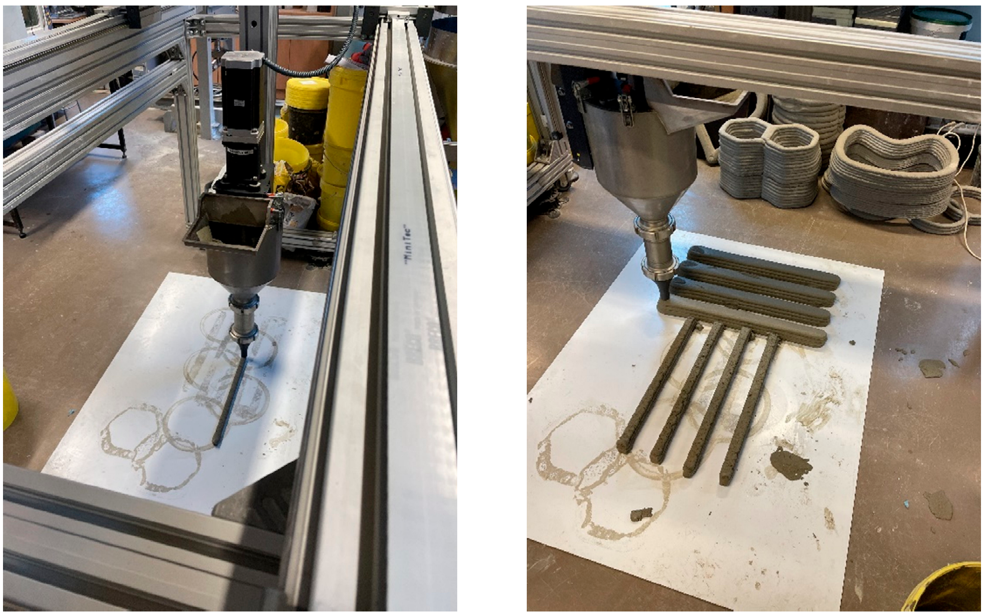

Figure 1. Test specimen printing process.

When specimens were printed, they were left overnight to set. At the same time, cast specimens were prepared. They were poured into a steel prismatic cast of 40 × 40 × 160 mm. A day later, cast specimens were unmolded, and printed specimens were cut to the same shape (40 × 40 × 160 mm) as the cast specimens. They all were placed in an aqueous environment for 25 days. After 25 days, all specimens were prepared for the creep and drying shrinkage tests.

The compressive strength was determined for four specimens (prismatic specimens 40 × 40 × 160 mm) out of each specimen type. The load was applied to the specimens for creep tests according to the determined compressive strength values. Compressive strength and creep and drying shrinkage (further in the text referred to as shrinkage) tests were conducted using the identical shape specimens so that creep specimens would not have shape factor impact (if the compressive strength specimens were larger or smaller than creep specimens) in the load that they were subjected on the test stands. All of the specimens intended for creep testing were loaded with 20% of the ultimate compressive strength value. Specimen placement into the creep test stand and shrinkage stand is shown in Figure 2.

(**a**)

(**b**)

Figure 2. The 3D-printed and cast cement composite shrinkage (**a**) and creep (**b**) test setup.

Creep and shrinkage tests were carried out for 28 days. Creep and shrinkage testing procedure, except testing time, was performed according to RILEM TC 107 recommendations [10]. The laboratory conditions for the creep and shrinkage tests were 24 ± 1 °C and 30 ± 3% relative humidity.

After creep and shrinkage tests to determine the reasons for inequal creep and shrinkage strains to the specimen sides, as well as to see the 3D-printed layer adhesion, quantitative image analysis was performed to the specimen's polished sections that were prepared and made according to the [11] used process.

3. Results and Discussion

The compressive strength was determined before the creep tests. Four specimens were used to determine compressive strength values for printed and cast specimens. The specimen's age at the time of testing was 28 days. The compressive strength values are shown in Figure 3.

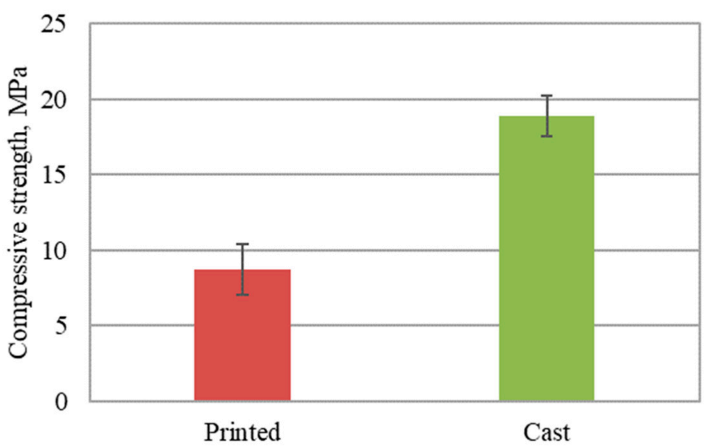

Figure 3. The 3D-printed and cast cement composite compressive strength values with measurement errors.

As visible from the compressive strength diagram, printed specimens loaded longitudinally to their layer placement exhibit more than two times lower compressive strength than cast specimens; furthermore, their standard measurement error is 17.9% larger than cast specimens.

Afterward, 28 day-long early creep and shrinkage tests were run, and the resulting readings are compiled in Figure 4.

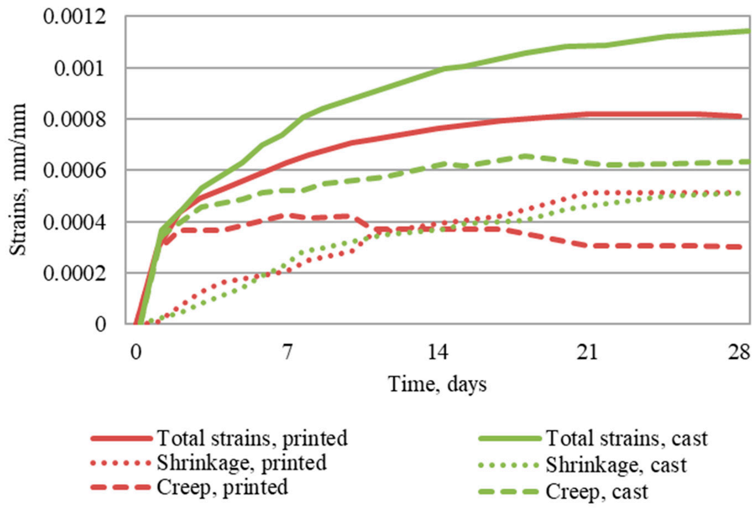

Figure 4. The 3D-printed and cast cement composite total recorded, creep, and shrinkage strains.

As it is clear from the curves in Figure 4, the shrinkage strains for printed and cast specimens are very close, or even identical. However, the creep strains have significant differences. Printed specimens show, at the peak values, 28.3% less creep strains. Additionally, the creep curve of printed specimens shows strain-decreasing relations starting from day 12 until day 28, while creep strains in cast specimens rise until day 18 and then exhibit a slight decrease. This implies that there must be some layer adhesion issue or that the load impact to the specimen resulted in the degradation of the structure. As the printed specimens have significantly lower compressive strength than cast specimens, it is necessary to calculate specific creep to see the creep strains without applied stress impact.

Specific creep values are calculated according to the equation, and the results are in Figure 5:

$$\chi_{cr}(t,t_0) = \frac{\varepsilon_{cr}(t,t_0)}{\sigma} = \frac{\varepsilon_{kop}(t) - \varepsilon_{sh}(t) - \varepsilon_{el}(t,t_0)}{\sigma} = \frac{1}{E_{cr}(t,t_0)} \tag{1}$$

where:

$\chi_{cr}(t,t_0)$ is the specific creep,
$\varepsilon_{cr}(t,t_0)$ is the creep strain,
$\varepsilon_{kop}(t)$ is the total strain,
$\varepsilon_{sh}(t)$ is the shrinkage strain,
$\varepsilon_{el}(t,t_0)$ is the elastic strain,
σ is the compressive stress,
and $E_{cr}(t,t_0)$ is the modulus of creep.

In Figure 5, it is clear that 3D-printed cement composites exhibit significantly higher specific creep; in other words, they are more willing to creep. On average, they have 32.8% higher specific creep than cast specimens. Furthermore, their specific creep appears within a couple of days, while it develops during the first 21 days of testing in cast specimens.

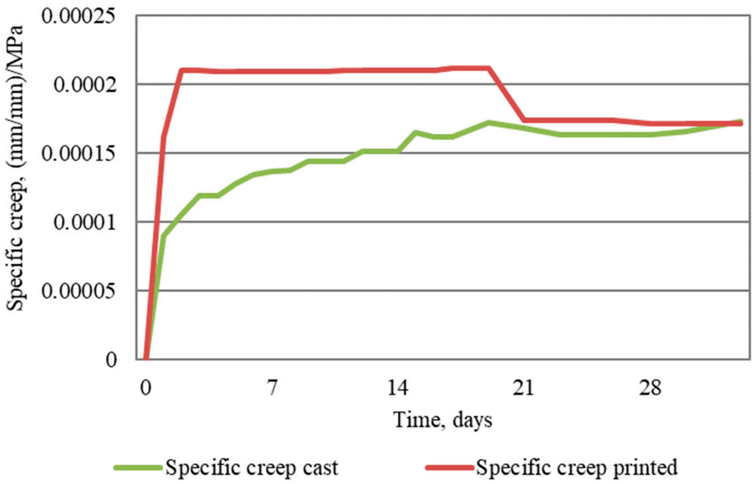

Figure 5. The 3D-printed and cast cement composite specific creep.

To further elaborate the assumption that printed specimens have some issues in the printed layers, the strain readings were divided into those that were measured to the top surface layer and those in which the surface consists of layer-side surfaces (placement and description shown in Figure 6).

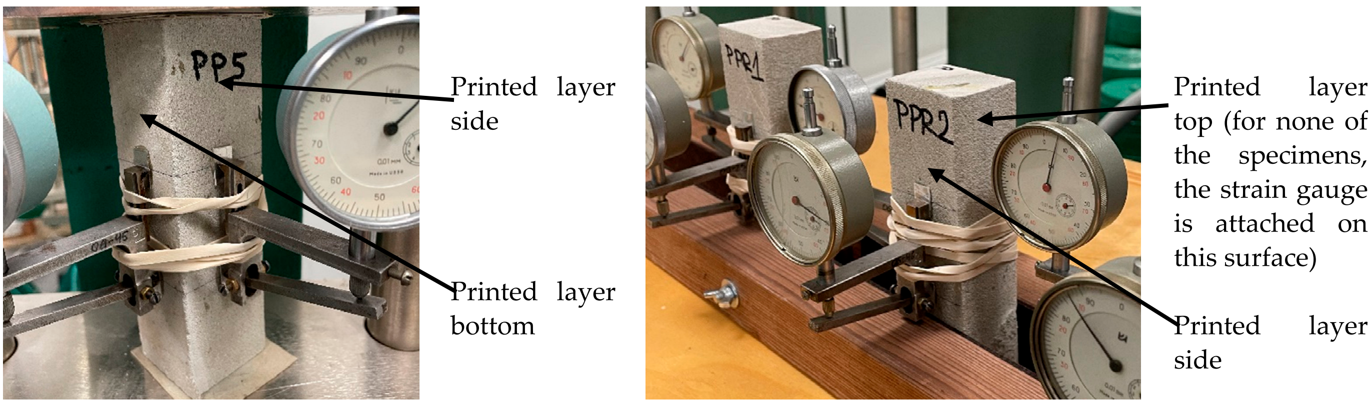

(**a**) (**b**)

Figure 6. The 3D-printed cement composite strain gauge placement on layer sides and surface for creep (**a**) and shrinkage (**b**) specimens.

The long-term shrinkage and creep strain curves according to strain gauge fitment are shown in Figure 7.

Here, it becomes clear that while long-term strain curves in the relation are similar, the creep strains and shrinkage strains are very different. While creep and shrinkage curves rise steadily to the layer top surfaces, the sides seem to have deterioration due to shrinkage. As the specimens were tested at the age of 28 days, the main shrinkage effect came from drying shrinkage. The shrinkage strain curves from the layer side surfaces lead to the conclusion that layers have been partially separated. To further elaborate, printed specimens after long-term tests were saturated in epoxy resin and used to make polished section specimens that then had their microstructure examined. It was determined that for all specimens, one side of the layer was more porous (see Figure 8) than the rest of the polished section surface.

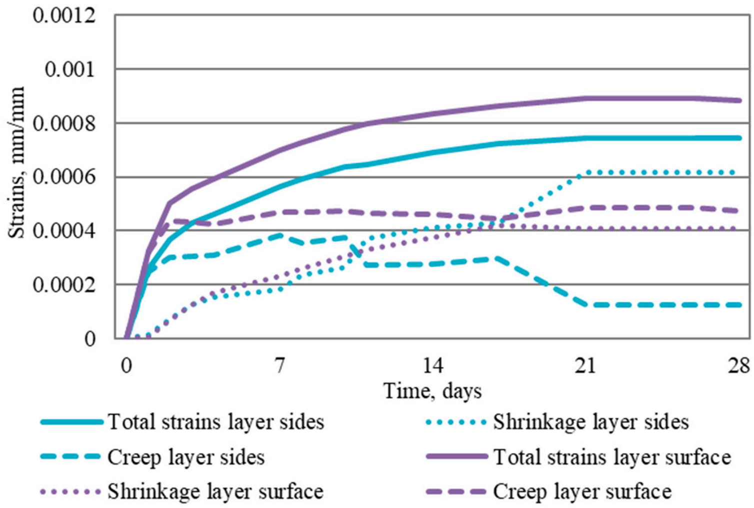

Figure 7. The 3D-printed cement composite total recorded, creep, and shrinkage strains according to strain gauge placement.

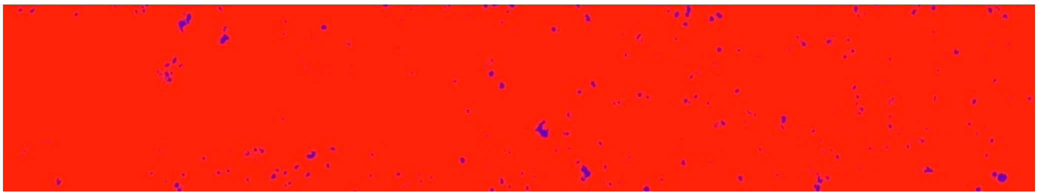

(**a**)

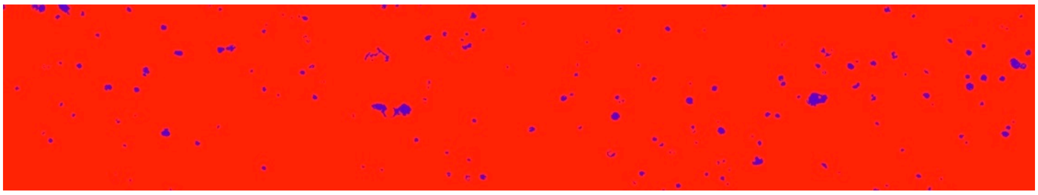

(**b**)

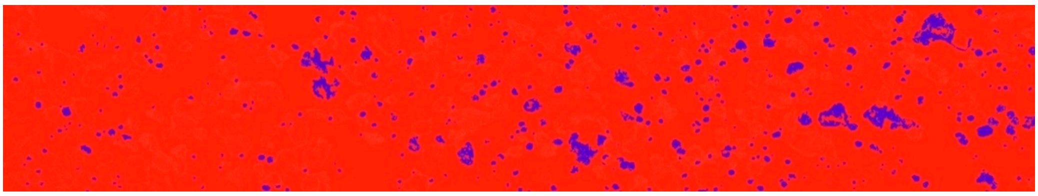

(**c**)

Figure 8. Quantitative image analysis images with matrix and filler part (red) and air void parts (blue) to the left side (**a**), middle part (**b**), and right side (**c**) of the specimen cross-section.

The specimens were printed using a plastic nozzle that had been printed on the plastic 3D printer. It had a stitched part that, as it turns out, frothed up part of the cement composite that interacted with this part of the nozzle. The model of the nozzle is shown in Figure 9. The white part in the model is the part where plastic layers are connected, and the stitch is developed.

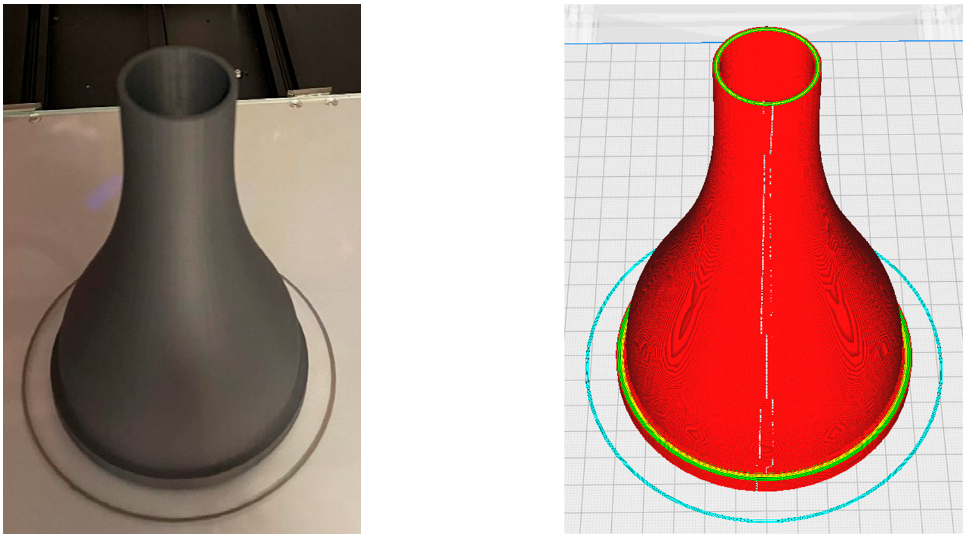

Figure 9. The 3D printer nozzle printed and modeled part.

4. Conclusions

Early-age creep and shrinkage property tests were performed on the prismatic specimens at the age of 28 days. The long-term property tests were carried out for 28 days. Prior to the long-term tests, compressive strength was determined for the cast and printed specimens. Following conclusions are:

1. According to the subjected stress state of the specimens, the printed cement composite specimens exhibit 53.7% lower compressive strength than cast cement composites. They also have a 17.9% higher standard error than cast specimens.
2. Printed specimens that have had load applied in the same way as the layers are laid show 28.3% fewer creep strains. Shrinkage strains are the same for printed and cast specimens.
3. Printed specimens are more prone to creep, as printed specimens' specific creep value is 32.8% higher on average than cast specimens.
4. Shrinkage strains in printed specimens have a significant role, and due to drying, shrinkage specimens show significant increases in shrinkage. It is very likely that this is due to the specifics of the used nozzle geometry. An increase in porosity in the specimen layer sides was observed. According to microstructure evaluation on specimen sides, there are 12% and 18% more pores to the shrinkage and creep specimens, correspondingly, than in the middle of the specimens.

Author Contributions: Conceptualization, R.G., P.P. and K.Z.; methodology, R.G. and K.Z.; software, R.G.; validation, P.P. formal analysis, R.G. and P.P.; investigation, R.G. and P.P.; resources, A.S. and G.B.; data curation, R.G. and P.P.; writing—original draft preparation, R.G.; writing—review and editing, R.G.; visualization, R.G.; supervision, A.S. and G.B.; project administration, R.G. and K.Z.; funding acquisition, R.G. All authors have read and agreed to the published version of the manuscript.

Funding: This publication was supported by Riga Technical University's Doctoral Grant program.

Institutional Review Board Statement: Not applicable.

Informed Consent Statement: Not applicable.

Data Availability Statement: Not applicable.

Acknowledgments: This work was supported by the European Social Fund within the Project No. 8.2.2.0/20/I/008 "Strengthening of PhD students and academic personnel of Riga Technical University and BA School of Business and Finance in the strategic fields of specialization" of the Specific Objective 8.2.2 "To Strengthen Academic Staff of Higher Education Institutions in Strategic Specialization Areas» of the Operational Programme «Growth and Employment". This work has been supported by the Latvian Council of Science within the scope of the project "Foamed Geopolymer Made by Additive Manufacturing for the Construction Technology Ap-plications (3D-FOAM)" No. project9608. Publication cost of this paper was covered with founds of the Polish National Agency for Academic Exchange (NAWA): "MATBUD'2023—Developing international scientific cooperation in the field of building materials engineering" BPI/WTP/2021/1/00002, MATBUD'2023.

Conflicts of Interest: The authors declare no conflict of interest.

References

1. Li, Z.; Hojati, M.; Wu, Z.; Piasente, J.; Ashrafi, N.; Duarte, J.P.; Nazarian, S.; Bilén, S.G.; Memari, A.M.; Radlińska, A. Fresh and hardened properties of extrusion-based 3D-printed cementitious materials: A review. *Sustainability* **2020**, *12*, 5628. [CrossRef]
2. Wong, K.V.; Hernandez, A. A Review of Additive Manufacturing. *ISRN Mech. Eng.* **2012**, *2012*, 1–10. [CrossRef]
3. Buswell, R.A.; Soar, R.C.; Gibb, A.G.F.; Thorpe, A. Freeform Construction: Mega-scale Rapid Manufacturing for construction. *Autom. Constr.* **2007**, *16*, 224–231. [CrossRef]
4. Wegrzyn, T.F.; Golding, M.; Archer, R.H. Food Layered Manufacture: A new process for constructing solid foods. *Trends Food Sci. Technol.* **2012**, *27*, 66–72. [CrossRef]
5. Nematollahi, B.; Xia, M.; Sanjayan, J. Current progress of 3D concrete printing technologies. In Proceedings of the 34th International Symposium on. Automation and Robotics in Construction and Mining, Taipei, Taiwan, 28 June–1 July 2017; pp. 260–267.
6. Zhang, J.; Wang, J.; Dong, S.; Yu, X.; Han, B. A review of the current progress and application of 3D printed concrete. *Compos. Part A Appl. Sci. Manuf.* **2019**, *125*, 105533. [CrossRef]
7. Baz, B.; Aouad, G.; Kleib, J.; Bulteel, D.; Remond, S. Durability assessment and microstructural analysis of 3D printed concrete exposed to sulfuric acid environments. *Constr. Build. Mater.* **2021**, *290*, 123220. [CrossRef]
8. Ding, T.; Xiao, J.; Zou, S.; Zhou, X. Anisotropic behavior in bending of 3D printed concrete reinforced with fibers. *Compos. Struct.* **2020**, *254*, 112808. [CrossRef]
9. Wang, L.; Tian, Z.; Ma, G.; Zhang, M. Interlayer bonding improvement of 3D printed concrete with polymer modified mortar: Experiments and molecular dynamics studies. *Cem. Concr. Compos.* **2020**, *110*, 103571. [CrossRef]
10. Acker, P.; Agullo, L.; Auperin, M.; Carol, I.; Carreira, D.J.; Catarino, J.; Chem, J.-C.; Chiorino, M.A.; Dougill, J.W.; Huet, C.; et al. Rilem Tc 107-Csp: Creep and Shrinkage Prediction Models: Principles of Their Formation Recommendation Measurement of time-dependent strains of concrete. *Mater. Struct.* **1998**, *31*, 507–512.
11. Gailitis, R.; Sprince, A.; Kozlovskis, T.; Radina, L.; Pakrastins, L.; Vatin, N. Long-Term Properties of Different Fiber Reinforcement Effect on Fly Ash-Based Geopolymer Composite. *Crystals* **2021**, *11*, 760. [CrossRef]